Journal of Petroleum Exploration and Production Technology (2021) 11:2075–2089
https://doi.org/10.1007/s13202-021-01165-7

ORIGINAL PAPER-EXPLORATION GEOPHYSICS

Well logging data interpretation for appraising the performance of Alam El-Bueib reservoir in Safir Oil Field, Shushan Basin, Egypt

Mohamed Mahmoud Elhossainy[1] · Ahmed Kamal Basal[2] · Hussein Tawfik ElBadrawy[1] · Sobhy Abdel Salam[1] · Mohammad Abdelfattah Sarhan[2]

Received: 5 March 2021 / Accepted: 8 April 2021 / Published online: 3 May 2021
© The Author(s) 2021

Abstract

This paper presents different well log data interpretation techniques for evaluating the reservoir quality for the sandstone reservoir of the Alam El-Bueib-3A Member in Safir-03 well, Shushan Basin, Egypt. The evaluation of the available well log data for the Alam El-Bueib-3A Member in this well indicated high quality as oil-producing reservoir between depths 8108–8133 ft (25 ft thick). The calculated reservoir parameters possess shale volume less than or equal to 9% indicating the clean nature of this sandstone interval, water saturation values range from 10 to 23%, and effective porosity varies between 19 and 23%. Bulk volume of water is less than 0.04, non-producing water (S_{Wirr}) saturation varies between 10 and 12%, and permeability ranges from 393 to 1339 MD reflecting excellent reservoir quality. The calculated BVW values are less than the minimum ($BVW_{min} = 0.05$) reflecting clean (no water) oil production, which was confirmed through the drill stem test (DST). The relative permeabilities to both water and oil are located between 0.01–0 and 1.0–0.5, respectively. The water cut is fairly low where it ranges between 0 and 20%. Additionally, the water saturation values are less than the critical water saturation ($S_{cw} = 29.5\%$) which reflects that the whole net pay will flow hydrocarbon, whereas the water phase will remain immobile. This was confirmed with reservoir engineering through the DST.

Keywords Well logging · Reservoir evaluation · Alam El-Bueib member · Safir Oil Field · Shushan Basin

Abbreviations

BIT	Bit size
CALX	Caliper
GR	Gamma ray
SPDH	Spontaneous potential
M2R9	Resistivity of un-invaded zone (Rt)
M2R3	Resistivity of transition zone (Rs)
RMSL	Resistivity of flushed zone (Rxo)
CNCF	Neutron porosity
ZDEN	Bulk density
PE	Photoelectric factor
IP	Interactive Petrophysics Software
AEB	Alam El-Bueib
PU	Porosity unit
K	Absolute permeability
S_{wirr}	Irreducible water saturation
BVW_{min}	Minimum bulk volume water
BVW	Bulk volume of water
S_{cw}	Critical water saturation
S_w	Water saturation
Φ	Porosity
Vsh	Shale volume
DST	Drill stem test
Ft	Feet
MD	Millidarcy
PHIT	Total porosity
PHIE	Effective porosity
R_w	Formation water resistivity
R_{mf}	Resistivity of mud filtrate
S_{wr}	Water saturation ratio
R_O	Resistivity of the wet zone

✉ Mohamed Mahmoud Elhossainy
Mohammed_Elhossainy@sci.kfs.edu.eg

[1] Geology Department, Faculty of Science, Kafrelsheikh University, Kafrelsheikh 33516, Egypt

[2] Geology Department, Faculty of Science, Damietta University, New Damietta City, Egypt

Introduction

The Western Desert represents one of the greatest productive hydrocarbon's provinces in the Egyptian territory. The Shushan Basin has a significant exploration potential in northern Western Desert (EGPC 1992). Safir Oil Field is located in the Shushan Basin between latitudes 30°35′–30°37′ N and longitudes 26°53′–26°55′ E as shown in Fig. 1. It represents one of the numerous hydrocarbon discoveries situated in this extremely faulted sedimentary basin. It is distinguished by high oil and gas accumulations which attracted the concern of the researchers and oil companies for hydrocarbons exploration. Khalda Petroleum Company was the main producer company since the discovery of Safir Oil Field in 1986.

The Alam El-Bueib Formation (Early Cretaceous; Barremian to Aptian) represents the main producing horizon in Safir Oil Field addition to the Kharita and Upper Bahariya formations (EGPC 1992).

This article aims at evaluating the petrophysical parameters for AEB-3A reservoir in Safir-03 well, Safir Field,

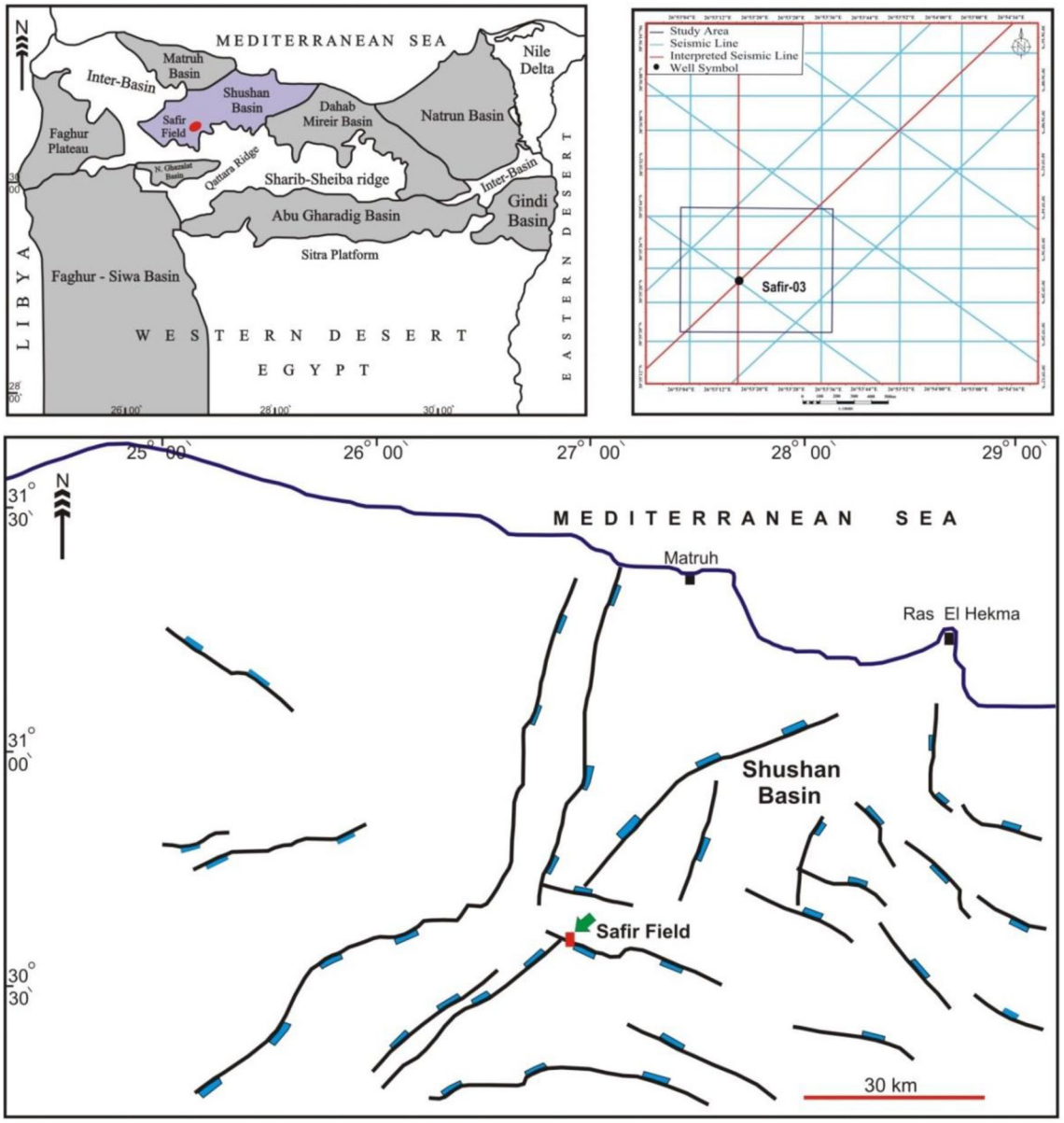

Fig. 1 Location map of Safir-03 well in Safir Field within Shushan Basin and seismic lines. The maps enlarged upper left and below show the main Mesozoic basins in the Western Desert and main structural elements and major faults in Shushan Basin, respectively (EGPC, 1992; Shalaby et al. 2012, 2014)

Western Desert in Egypt. The available data include a suite of well log and number of seismic lines. The petrophysical parameters include shale volume (Vsh), porosity (Φ), water saturation (S_w), critical water saturation (S_{cw}), bulk volume of water (BVW), minimum bulk volume water (BVW_{min}), irreducible water saturation (S_{wirr}) and absolute permeability (K).

Geological setting

Moustafa (2008) concluded that the sedimentary basins of the northern Western Desert including Shushan Basin were subjected to tectonic inversion during the Upper Cretaceous. Moustafa 2008; Sarhan 2017; Sarhan et al. 2017a and b; Sarhan and Collier 2018; Sarhan 2019 attributed the NE-SW trending anticlines which were produced in northern Western Desert to the NW movement of the African Plate relative to Laurasian Plate.

Shushan Basin is a half-graben basin (El Shazly 1977; Hantar 1990). It was developed as a result of the initial origin of the Neo-Tethys Sea and continued as a depocenter throughout most Cretaceous (Metwalli and Pigott 2005). It lies within the unstable shelf tectonic zone in Egypt (Said 1962) and bounded by the Umbarka Platform to the north and by the Qattara Ridge to the south (Alsharhan and Abd El-Gawad 2008).

In the North Western Desert, the lithostratigraphic section comprising Shushan Basin contains thick sedimentary succession that ranges from Paleozoic to Paleogene (Fig. 2). This sequence comprises of clastics depositional cycles alternating with carbonates (EGPC 1992).

The Lower Cretaceous period witnessed the sedimentation of a regressive phase and marginal marine clastics of Alam El Bueib (AEB) Formation. The transgressive phase represents a shallow sea over the north Western Desert, where the carbonate unit of the Alamein Formation was deposited during the Aptian age. The Albian is represented by another regressive phase, when the North Western Desert received the fluvial input (mainly coarse sands) of the Kharita Formation which coming from the south (Said 1990).

The main reservoir of Shushan Basin is the Lower Cretaceous (AEB Formation) which represents one of the generality productive formations in the Western Desert, predominantly in the concession of Khalda Oil Company (Schlumberger 1995). The AEB Formation is composed of fine to coarse grains clastics that conformably overly the Masajed Formation (Upper Jurassic carbonates) and underlay the Alamein Dolomite (Fig. 2). The AEB Formation was subdivided into six units based on the lithological variation, these units arrange from top to base; AEB-1, AEB-2, AEB-3, AEB-4, AEB-5 and AEB-6. Also, AEB-3 unit is further subdivided into six sub-units from top to base: A, C, D, E, F and G (Hantar 1990).

Data and techniques

The available data include (20) two-dimensional reflection vertical seismic sections that cover the study area in addition to the well logging dataset for Safir-03 well (Fig. 1). The accessible well log data in Safir-03 well include bit size (BIT), caliper (CALX), gamma ray (GR), spontaneous potential (SPDH), resistivity (M2R9, M2R3 and RMSL), neutron porosity (CNCF), density (ZDEN), density correction (ZCOR) and photoelectric factor (PE). The logging analysis was carried out using Senergy Software Interactive Petrophysics program (IP) (version 3.6). The whole abbreviations stated in this study are listed at the begning of the paper.

The structural setting of AEB-3A Member has been deducted from the interpretation of the available 2D seismic lines. However, the formation evaluation for the sandstone of the AEB-3A Member to be a potential hydrocarbon reservoir in Safir Field was based on qualitatively and quantitatively interpretation.

Results

Seismic data interpretation

The seismic reflector (horizon) that represents Alam El-Bueib 3A Member has been easily detected on the existing seismic profiles because it is characterized by strong amplitude and high continuity (Fig. 3). The traced horizon on the seismic sections exhibits a clear raised fault block relative to their surroundings bounded by two normal faults. This horst has been clearly notable in Fig. 3.

Well-log interpretation (qualitative and quantitative)

Qualitative interpretation

The interpretation of the well log curve shapes and their relative positions to each other represent the key for judging the existence of any possible reservoir and for discrimination between hydrocarbon and wet productive intervals.

Figure (4) represents a complete set of log data for AEB-3A Member in Safir-03 well in the form of Triple Compo format as one option of the Interactive Petrophysics (IP) software. The visual examination of the available well log data for the AEB-3A Member in the Safir-03 well indicates that the interval from 8108 to 8133 ft has very interesting

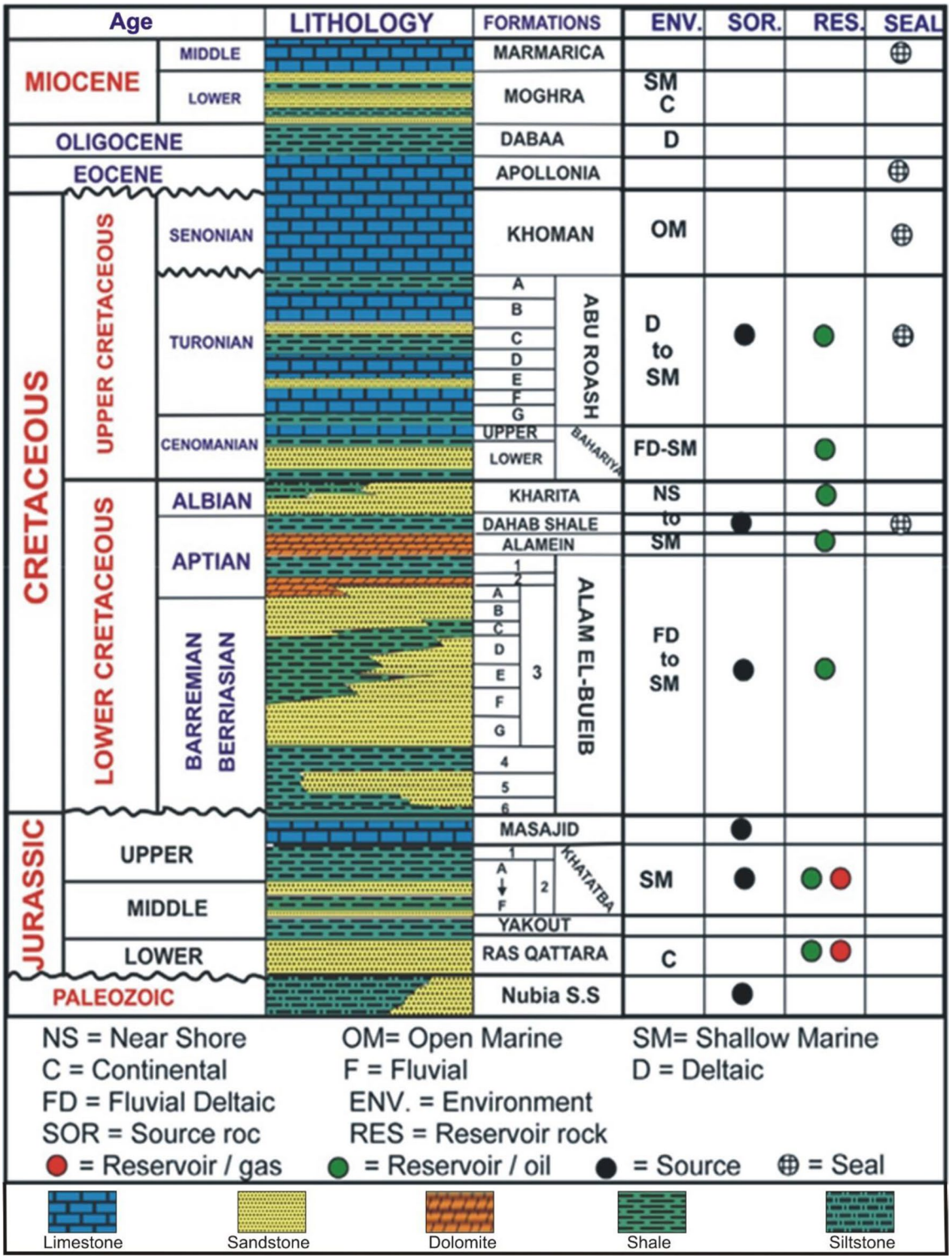

Fig. 2 General lithostratigraphic column of the Western Desert of Egypt (modified from Schlumberger 1995)

log characters and optimistic log curve shapes (Fig. 4). This interval reflects good hole conditions as indicated by the caliper log (CALX) (blue color, track number 1) that reads borehole diameter values that are equal to the bit size (BIT) or even less than it.

Neutron curve (CNCF) is displayed on the right side to the density curve (ZDEN) on track number (5) and PE

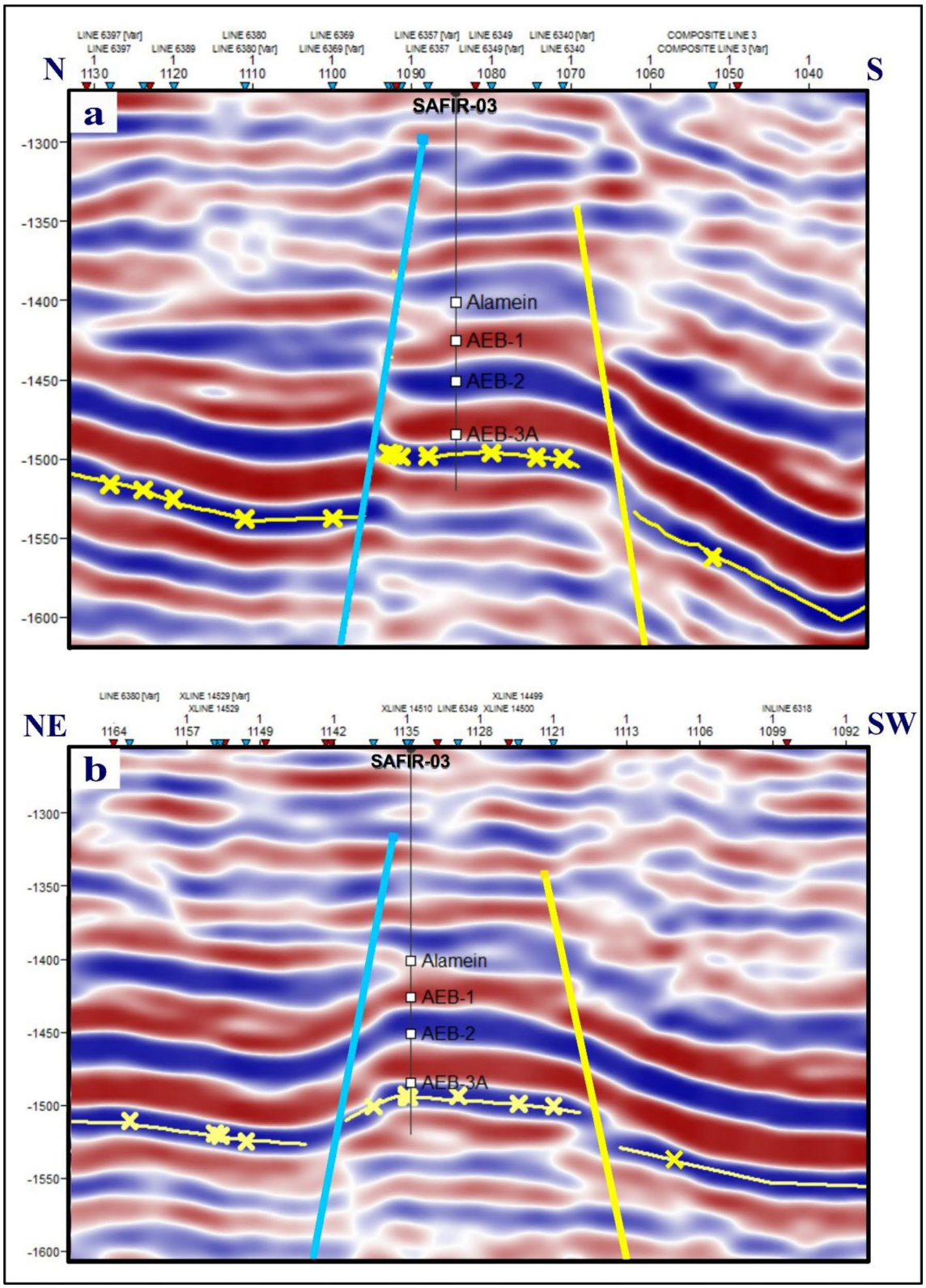

Fig. 3 The picked horizon of AEB-3A Member (yellow color) as tied to Safir-03 well. (**a**) S–N Xline 14499 seismic profiles. (**b**) NE-SW composite line 1 seismic profiles

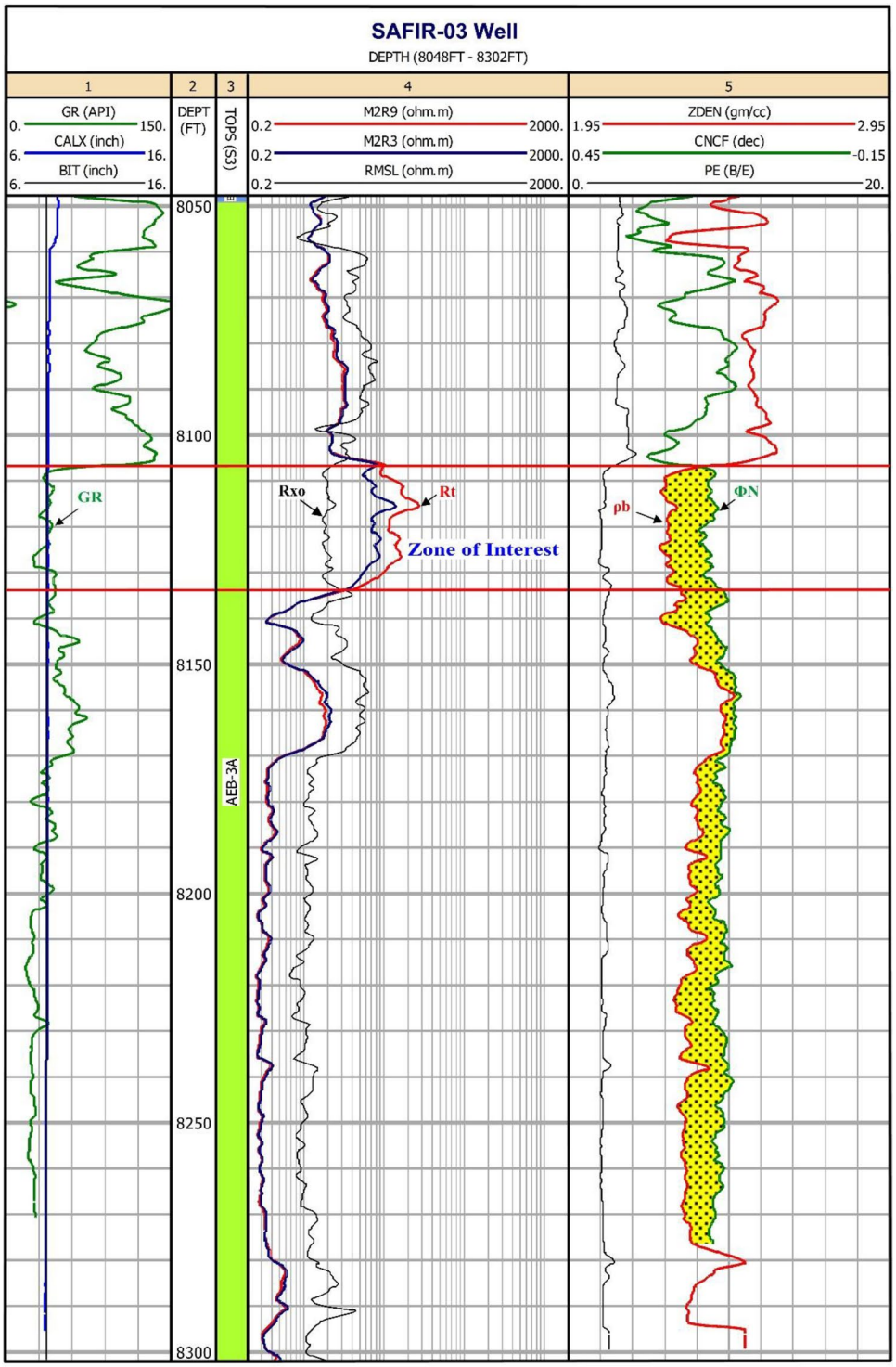

Fig. 4 Well log data Triple Compo as displayed on the IP Software for AEB-3A Member, Safir-03 well, Safir Field, North Western Desert

reading of about 2 b/e confirms the sandstone matrix. Low gamma ray reading (Track 1) reflects a clean sandstone interval. The plotted points of this interval are clustered around the sandstone line that has porosity ranging between 21 and 25 PU based on the neutron—density cross-plot (Fig. 5). Also, the grain size in the examined AEB-3A reservoir indicates that the majority of the sand grains within this interval are coarse grains based on the analysis of the cross-plot of the porosity against water saturation (Fig. 6).

The former interpretation of the well logging data indicates that the uppermost interval of AEB-3A Member (between 8108 and 8133 ft) displays certain signs of movable hydrocarbons. The resistivity curves of this interval also display clear positive separation (M2R9 > M2R3

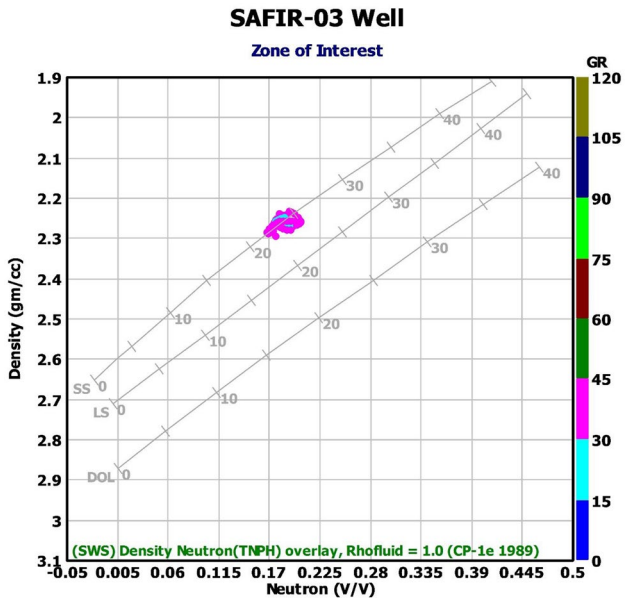

Fig. 5 Neutron—density cross-plot (Schlumberger, 1972) of AEB-3A Member, Safir-03 borehole displaying that the reservoir interval is predominated by sandstone matrix

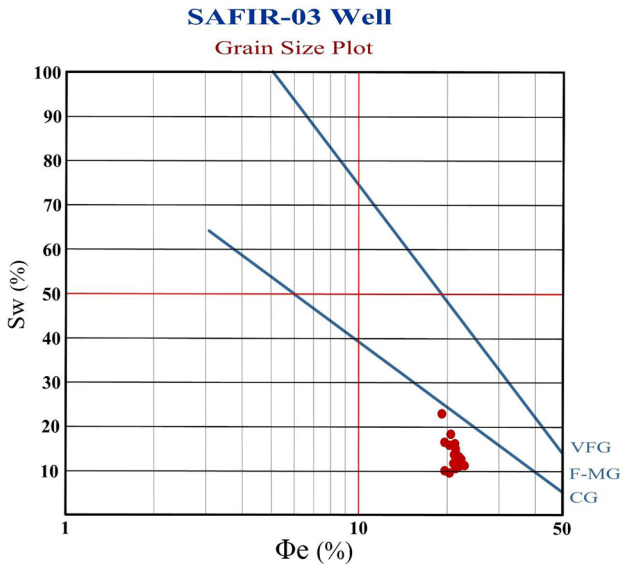

Fig. 6 Porosity—water saturation cross-plot (Asquith and Gibson, 1982) displays the distribution of the grain size of the AEB-3A sandstone reservoir

> RMSL) (as shown in Track 4) indicating the presence of invasion profile, which reflects good porosity and permeability. The porosity logs (CNCF and ZDEN) show high porosity values that range from 21 to 25%. The minimum content of shale is indicated by the lowest gamma ray reading.

Quantitative interpretation

Based on these prior diagnoses, furthermore calculations were done for the expected pay interval of AEB-3A Member between 8108 and 8133 ft. These calculations include the following petrophysical parameters: shale volume (Vsh), total porosity (PHIT), effective porosity (PHIE), water saturation in the un-invaded zone (S_w), bulk volume of water (BVW), irreducible water saturation (S_{wirr}), absolute permeability (K), critical water saturation (S_{cw}) and minimum bulk volume of water (BVW_{min}). The quantitative evaluations of the examined interval were calculated based on Archie model (Archie 1942), and the gained results were displayed in Table (1).

Water Saturation (S_W) Water saturation of the virgin zone (S_w) is fundamental parameter for any further quantitative interpretation and reservoir evaluation. As the reservoir is clean inter-granular porosity sandstone, Archie model (1942) is used as follows:

$$\left(S_w\right)^n = \frac{aRw}{\Phi^m \times Rt} \quad (1)$$

The resistivity of the formation water (R_w), resistivity of the virgin zone (true resistivity, R_t) and porosity (Φ) represent the fundamental parameters needed for calculating the reservoir water saturation (S_w). While the true resistivity (R_t) and porosity (Φ) are easily obtained directly from the log curve as described above, the formation water resistivity (R_w) cannot be directly picked on the logs.

The 100% water saturated zone is located directly below about depth equals 8133 feet where Rt suddenly lowered to 0.3 $\Omega m^2/m$ (Fig. 4). This value will be considered to represent R_o. The water zone has the same matrix as that of the reservoir with average porosity equals 19%. The connate water resistivity (R_w) can then be obtained by applying Archie equation ($R_o = F \times R_w$) with $F = 1/\Phi^2$. In this case, R_w is calculated to be equals 0.01 $\Omega m^2/m$. This value matched well with 0.019 $\Omega m^2/m$ obtained through the analysis of formation water samples under the same reservoir conditions in the majority of fields of Khalda Petroleum Company.

According to the above discussion, the average reservoir water saturation (S_w) can then be calculated with average effective porosity of 0.21 and resistivity (R_t) equals 14 $\Omega.m^2/m$. The calculated average water saturation equals 13%. In addition, the flushed zone water saturation (S_{xo}) can also be calculated using Archie equation by replacing R_t and R_w with R_{xo} and R_{mf}, respectively, as:

$$(S_{xo})^n = \frac{aRmf}{\Phi_m \times Rxo} \quad (2)$$

The mud filtrate resistivity (R_{mf}) can be determined for zone which have S_w equals 100% ($R_{mf} = \Phi 2 \times R_{xo}$). The shallow resistivity (R_{xo}) opposite 100% wet zone equals 1 Ω.m^2/m with (0.19) porosity. Applying this technique gives R_{mf} value of about 0.036 Ω.m^2/m. It is interesting to notice that this value 0.036 is very close to 0.034 that obtained from well header (0.1 Ω.m^2/m @ 60 °F) after adjusting to formation temperature (Tf = 190°F). In Fig. 7 by locating the resistivity value, 1 Ω.m^2/m, on the scale

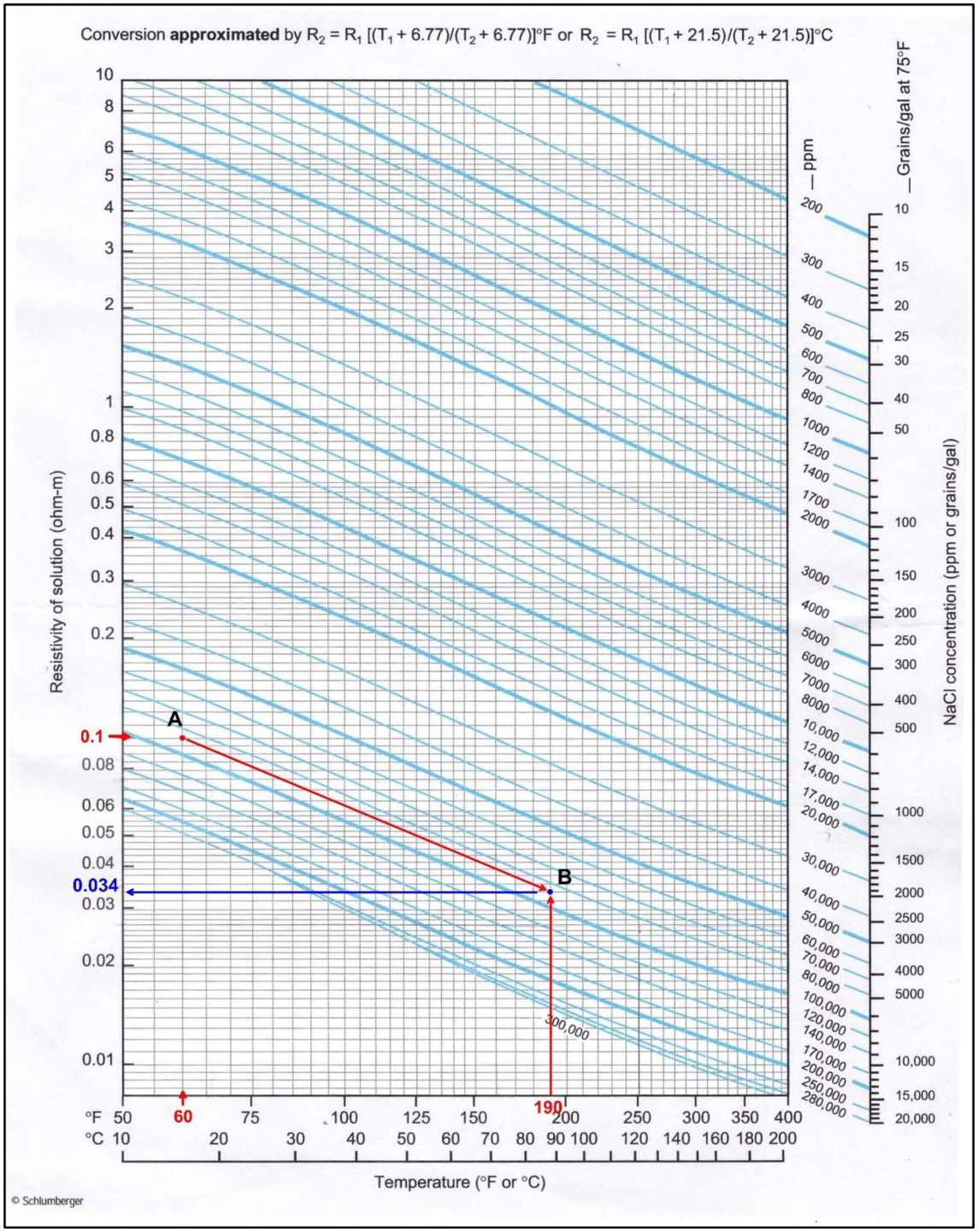

Fig. 7 Chart for adjusting the mud filtrate resistivity (R_{mf}) for formation temperature (Schlumberger, 1986, Figure Gen-9)

to the left of the graph and move horizontally to the right along the 1 $\Omega.m^2/m$ line until the vertical line representing a temperature of 60 °F (from the bottom of the graph) is met (point A on the chart). Then move parallel to the constant salinity line (diagonal) to the point where it intersects the vertical line representing a temperature value of 190 °F (point B on the graph). From point B, follow the horizontal line to the left to determine the resistivity of the mud filtrate at the desired temperature (0.034 $\Omega.m^2/m$ @ 190°F). Consequently, the average water saturation in flushed zone (S_{xo}) has been calculated in the pay zone using average effective porosity of 0.21 and average shallow resistivity (R_{xo}) of 2 $\Omega.m^2/m$. The results show that S_{xo} equals 64% (i.e., the movable hydrocarbon is 64% and the residual hydrocarbon is 36%) (Table 1).

The water saturation can be calculated by means of ratio method (S_{wr}) as (Asquith et al. 2004) is:

$$S_{wr} = \left(\frac{\text{Rxo/Rt}}{\text{Rmf/Rw}}\right)^{0.625} \tag{3}$$

where S_{wr} = water saturation ratio, R_{xo} = shallow resistivity, R_t = true formation resistivity, R_{mf} = resistivity of mud filtrate, R_w = connate water resistivity.

It is important here to notice that the calculated water saturations using Archie (Swa) and ratio (Swr) are about equal each other (Table 1) which mean that all values determined (S_w, R_t and R_{xo}) are correct (Asquith et al. 2004).

Pickett cross-plot The Pickett cross-plot, introduced by Pickett (1972), represents a graphical representation of Archie's model. It is constructed by representing the deep resistivity (R_t) on the horizontal axis and the porosity (Φ) at the vertical axis on a logarithmic Plot. This results in a linear equation as:

$$y = mx + b \tag{4}$$

$$\log \Phi = -\frac{1}{m}\log\left(R_t\right) - n\log\left(S_w\right) + \log\left(aR_w\right) \tag{5}$$

Using logarithmic scales for both axes, plotting the true resistivity (R_T) on the horizontal axis and porosity (Φ) on vertical axis, the parallel lines that represent the water saturation (S_w) can be drawn. The S_W for any plotted point can be read directly. This technique depends on the perception that the true resistivity is dependent on porosity (Φ), water saturation (S_w) and the factor of cementation (m). The 100% water saturation line represents the wet resistivity (R_O). The line has a slop of (-1/m) and intercepts the vertical scale, at porosity equals unity, where a (R_w) can be read on the resistivity scale.

The plotted points representing AEB-3A reservoir in Safir-03 well (Fig. 8) are clustered below 25% S_w line indicating oil production and matches very well with the calculated water saturation values above.

Bulk Volume of Water and Irreducible Water Saturation Buckles (1965) represented a graphical technique depending on plotting porosity (Φ) versus water saturation (S_w). When the bulk volume of water ($\Phi x S_W$) is constant (or almost constant), the plotted points will follow specific hyperbolic curve through this graph. In this case, the reservoir is said to be at irreducible state and the water in the virgin zone will not move and caught on the grain's surfaces by the capillary force. Consequently, the reservoir will produce only oil. The irreducible water saturation (Swirr) is of supreme importance for evaluating the performance of the reservoir and its quality. This parameter is needed for applying any model for calculating permeability from well log data. It can be read directly from Buckles plot.

Figure 9 represents Buckles plot for AEB-3A reservoir in Safir-03 well. The majority of the plotted points followed 0.025 BVW hyperbolic curve. As this reservoir described as sandstone, it can be concluded that it is at irreducible state (Table 1). The irreducible status in this reservoir may be also affected by the presence of amount of shale matrix which lead to the increase in capillary pressure. This capillary pressure holds the water molecules and prevent water to flow through the production process.

Asquith and Gibson (1982) presented the most popular relation to calculate the S_{wirr} for a particular zone using the formation factor (F) as:

$$S_{wirr} = \sqrt{\frac{F}{2000}} \tag{6}$$

It is important here to mention that this relation calculates the approximate and theoretical values and is valid only for constructing cross-plots to qualitatively evaluate the relative permeabilities (Kr) and water cut (WC).

Relative permeability (Kr) and water cut (WC) The main concern for any log analyst is the amount and type of fluid which will be produced. Accordingly, it is of prime importance to compare relative permeabilities to both oil and water (K_{ro} and K_{rw}, respectively), and the accompanying water cut (WC). As stated above, the irreducible water saturation ($S_W$irr) is the cornerstone for evaluating these parameters. In this article, Eq. (6) will be applied. In this concern, Schlumberger (1986) presented a number of charts representing graphically the relation between $S_W$irr versus SW. The following section represents application of such technique for AEB-3A reservoir in Safir-03 well.

Table 1 Well logging data and their output analysis of AEB-3A reservoir, Safir-03 borehole

Depth	Input well log data									Output results												
	GR	CALX	RMSL	M2R3	M2R9	ZDEN	CNCF	PE	VCL	Φ NDxp	PHIE	PHIT	SW	BVW	Swr	Swirr	K (Timur)	Sxo	Sh	Shr	MOI	Shm
(FT)	API	IN	Ω.m	Ω.m	Ω.m	gm/cc	Dec	B/E	Dec	Dec	Dec	Dec	Dec		Dec	Dec	MD	Dec	Dec	Dec	Sw/Sxo	Dec
8108	40.03	8.56	1.80	5.96	9.16	2.30	0.18	2.23	0.07	0.22	0.20	0.22	0.17	0.03	0.16	0.11	591.37	0.71	0.83	0.29	0.23	0.54
8109	34.99	8.55	1.79	5.74	10.11	2.26	0.18	2.18	0.05	0.23	0.21	0.23	0.15	0.03	0.15	0.11	736.38	0.68	0.85	0.32	0.22	0.53
8110	36.32	8.57	1.98	6.80	13.47	2.25	0.19	2.20	0.06	0.24	0.22	0.24	0.12	0.03	0.14	0.10	1098.72	0.61	0.88	0.39	0.20	0.49
8111	41.46	8.57	1.99	7.98	17.38	2.26	0.19	2.26	0.08	0.24	0.21	0.24	0.11	0.02	0.12	0.11	738.85	0.64	0.89	0.36	0.18	0.53
8112	43.46	8.57	1.91	7.31	16.80	2.25	0.18	2.27	0.09	0.24	0.21	0.24	0.12	0.03	0.12	0.11	738.85	0.65	0.88	0.35	0.18	0.54
8113	40.03	8.56	2.02	7.64	17.38	2.25	0.19	2.29	0.07	0.24	0.22	0.24	0.11	0.02	0.12	0.10	1095.61	0.61	0.89	0.39	0.18	0.50
8114	39.54	8.55	2.04	9.38	20.29	2.26	0.19	2.28	0.07	0.24	0.21	0.24	0.11	0.02	0.11	0.11	738.85	0.63	0.89	0.37	0.17	0.53
8115	40.92	8.55	2.46	13.21	26.68	2.27	0.18	2.27	0.08	0.23	0.20	0.23	0.10	0.02	0.10	0.11	593.59	0.61	0.90	0.39	0.16	0.51
8116	38.38	8.56	2.15	13.00	24.83	2.29	0.17	2.10	0.07	0.22	0.20	0.22	0.10	0.02	0.10	0.11	593.59	0.65	0.90	0.35	0.16	0.55
8117	33.45	8.57	1.92	9.01	16.41	2.27	0.18	1.95	0.05	0.23	0.21	0.23	0.12	0.03	0.12	0.11	738.85	0.65	0.88	0.35	0.18	0.54
8118	32.51	8.57	1.74	7.13	12.33	2.26	0.18	2.02	0.05	0.23	0.21	0.23	0.14	0.03	0.13	0.11	738.85	0.68	0.86	0.32	0.20	0.55
8119	40.36	8.57	1.77	7.49	12.14	2.26	0.19	2.07	0.07	0.24	0.21	0.23	0.14	0.03	0.14	0.11	738.85	0.68	0.86	0.32	0.20	0.54
8120	42.44	8.58	1.90	7.45	11.95	2.26	0.20	2.07	0.08	0.24	0.21	0.24	0.14	0.03	0.14	0.11	738.85	0.66	0.86	0.34	0.21	0.52
8121	39.95	8.57	1.76	7.25	11.84	2.26	0.20	2.09	0.07	0.24	0.22	0.24	0.13	0.03	0.14	0.10	1095.61	0.65	0.87	0.35	0.20	0.52
8122	38.17	8.56	2.03	8.72	14.65	2.27	0.19	2.08	0.07	0.24	0.21	0.23	0.12	0.03	0.13	0.11	738.85	0.63	0.88	0.37	0.20	0.51
8123	38.89	8.58	1.85	8.97	15.58	2.27	0.20	2.08	0.07	0.24	0.22	0.24	0.12	0.03	0.12	0.10	1095.61	0.63	0.88	0.37	0.18	0.52
8124	39.26	8.59	1.73	7.87	14.13	2.24	0.20	2.07	0.07	0.25	0.23	0.25	0.12	0.03	0.12	0.10	1339.56	0.63	0.88	0.37	0.18	0.51
8125	32.33	8.58	1.83	8.20	15.06	2.24	0.19	2.04	0.05	0.25	0.23	0.24	0.11	0.03	0.12	0.10	1339.56	0.61	0.89	0.39	0.18	0.50
8126	27.64	8.58	2.06	8.83	16.33	2.26	0.18	1.98	0.03	0.24	0.22	0.23	0.11	0.02	0.12	0.10	1095.61	0.60	0.89	0.40	0.19	0.49
8127	25.12	8.58	2.19	8.77	16.08	2.27	0.19	1.94	0.02	0.23	0.22	0.23	0.11	0.02	0.13	0.10	1095.61	0.58	0.89	0.42	0.19	0.47
8128	26.73	8.58	1.89	6.97	12.71	2.26	0.19	1.93	0.03	0.24	0.22	0.23	0.13	0.03	0.14	0.10	1095.6	0.63	0.87	0.37	0.20	0.50
8129	30.49	8.57	2.23	6.27	11.27	2.27	0.18	2.43	0.04	0.23	0.21	0.23	0.14	0.03	0.16	0.11	738.85	0.61	0.86	0.39	0.23	0.46
8130	44.88	8.56	1.90	5.64	9.93	2.28	0.19	2.42	0.09	0.23	0.20	0.23	0.16	0.03	0.16	0.11	593.59	0.69	0.84	0.31	0.23	0.53
8131	44.41	8.56	1.76	5.17	8.57	2.26	0.19	2.15	0.09	0.24	0.21	0.24	0.16	0.03	0.17	0.11	738.85	0.68	0.84	0.32	0.24	0.52
8132	44.27	8.57	1.94	4.59	6.77	2.26	0.18	2.44	0.09	0.23	0.21	0.23	0.18	0.04	0.20	0.11	738.85	0.65	0.82	0.35	0.28	0.47
8133	45.00	8.58	2.47	4.09	5.27	2.29	0.17	2.65	0.09	0.22	0.19	0.22	0.23	0.04	0.24	0.12	393.36	0.64	0.77	0.36	0.36	0.41
Av	38		2	8	14				0.07	0.235	0.21	0.23	0.13	0.03	0.13	0.11	845	0.64	0.87	0.36		0.51

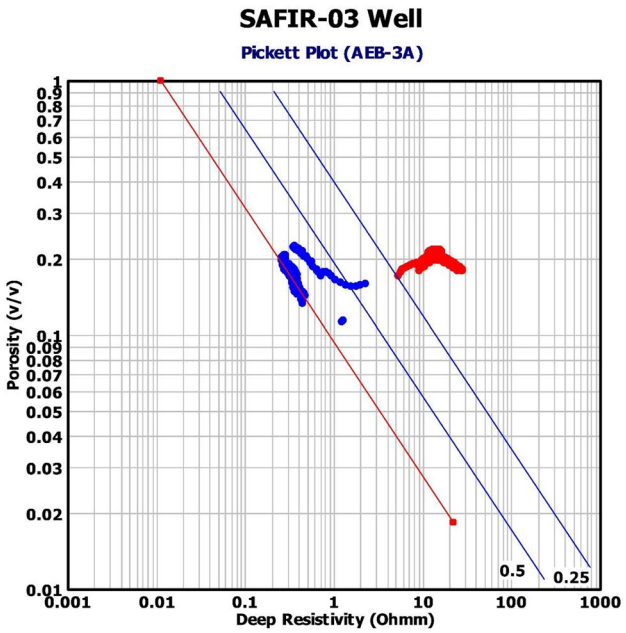

Fig. 8 Pickett plot for AEB-3A sandstone reservoir in Safir-03 borehole. The red points that are plotted below the 25% Sw line represent the pay interval

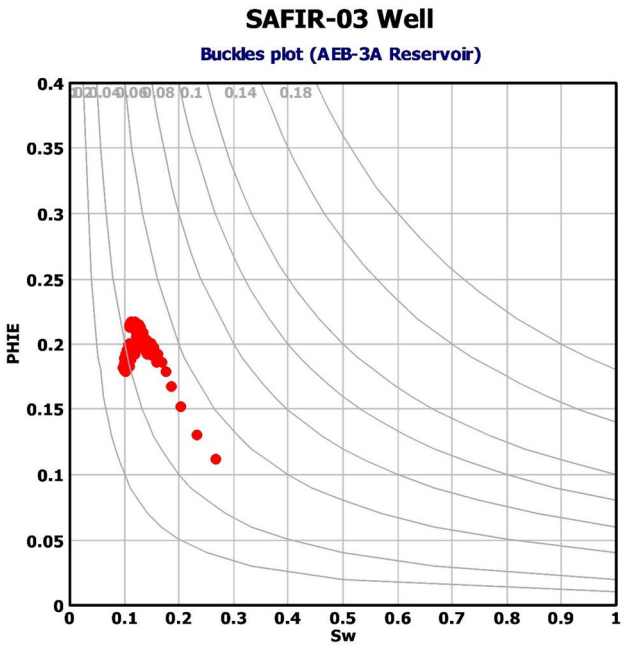

Fig. 9 Porosity versus water saturation (Buckles plot) for AEB-3A reservoir. The plot shows that the points follow the 0.035 hyperbola of the bulk volume of water (BVW), which indicates that the reservoir is producing free-water oil

Figure 10 represents relative permeabilities to water (K_{rw}) for each zone. The plotted points are clustered below 0.01 relative permeability to water. In addition, there are many

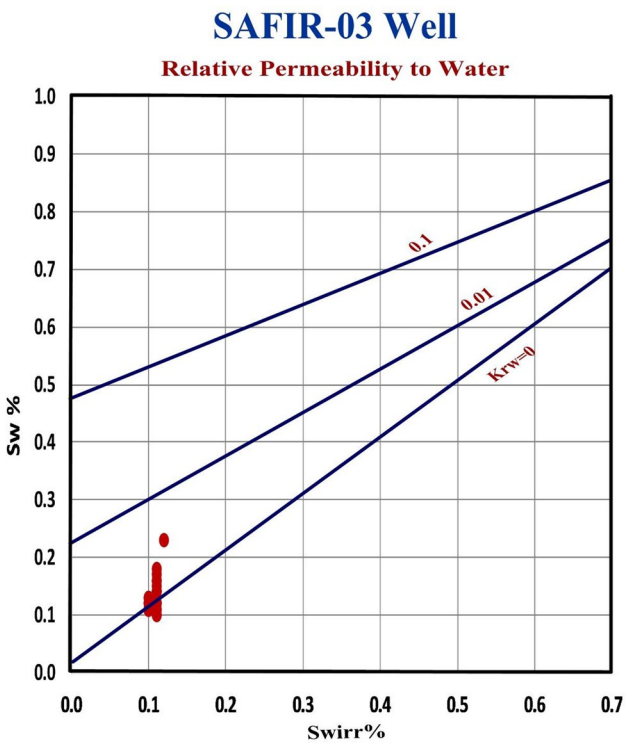

Fig. 10 Water saturation (S_w) against irreducible water saturation (S_{wirr}) plot (Asquith and Gibson, 1982) to determine relative permeability to water (K_{rw}) of the AEB-3A reservoir, Safir-03 well

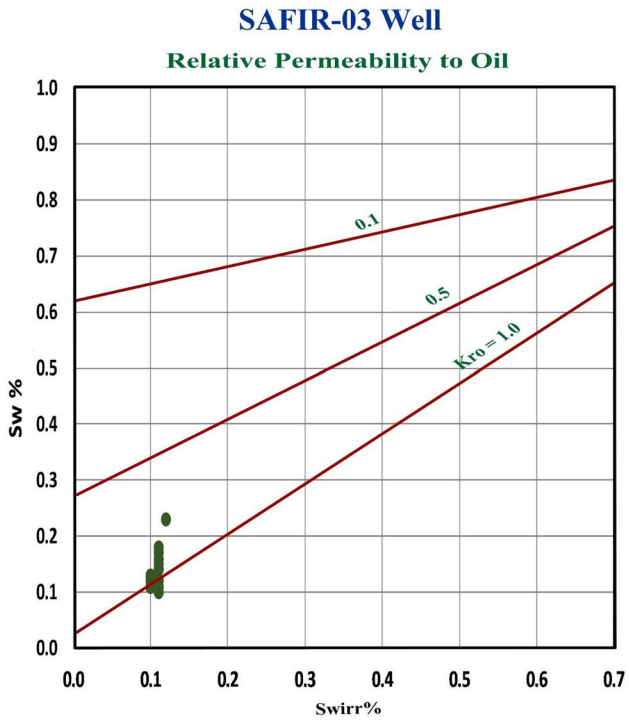

Fig. 11 Water saturation (S_w) versus irreducible water saturation (S_{wirr}) plot (Asquith and Gibson, 1982) to determine relative permeability to oil (K_{ro}) for AEB-3A reservoir, Safir-03 well

points plotted on and even below zero K_{rw}. This very low relative permeability to water reflects free water-producing reservoir (i.e., at irreducible state).

Figure 11 represents the different relative permeability to oil (K_{ro}) lines based on plotting $S_W$irr versus SW. The plotted points on this plot are clustered around 1 ($K_{ro} = 100\%$) line. This indicates that AEB-3A reservoir in Safir-03 well is expected to produce 100% oil. Points plotted with increasing distance from 1Kro line indicate zones which will produce some water.

The water cut (WC) cross-plot for the study reservoir (Fig. 12) shows that the plotted points clustered between 0 and 20% WC. This means that this reservoir has zones which will produce only oil in addition to another zones which will produce oil and water (less than 20%).

Absolute permeability (K) All log-derived permeability models are only valid for estimating permeability (K) in the reservoirs under irreducible state conditions (i.e., $S_w = S_{wirr}$). Absolute permeability (K) of the pay zone in AEB-3A reservoir was estimated using the following formula (Timur 1968):

$$K^{1/2} = 100\left(\frac{\Phi^{2.25}}{S_{\text{wirr}}}\right) \tag{7}$$

Table 1 summarizes the obtained permeability values for AEB-3A reservoir in Safir-03 well. It is clear that this reservoir possesses excellent permeability which ranged between 393 and 1339.5 MD with 845MD as average. This confirms good quality for AEB-3A reservoir in Safir-03 well.

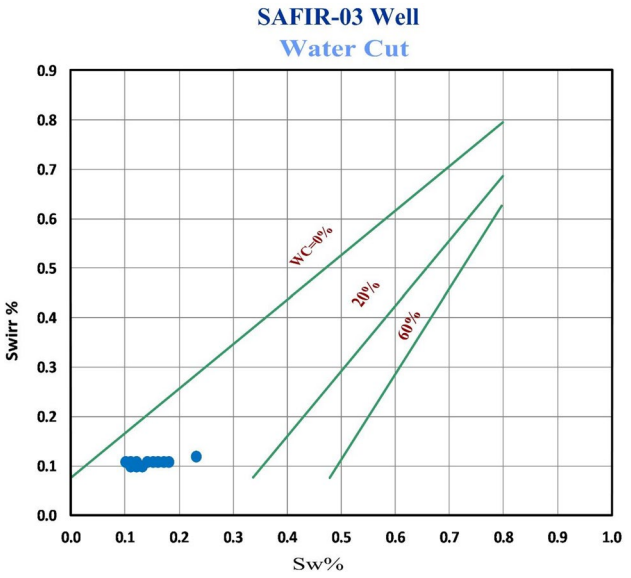

Fig. 12 Irreducible water saturation against water saturation plot (Asquith and Gibson, 1982) for estimating the percentage of water cut for the AEB-3A reservoir, Safir-03 well

Critical water saturation (S_{CW}) Critical water saturation (S_{cw}) is a percent of water above which the reservoir will begin to produce water in addition to oil. The ability of zones to produce oil depends on their relative permeability to oil and saturation (S_o). If the relative permeability to water (K_{rw}) is higher than that to oil (K_{ro}) as well as the water saturation (S_w) higher than the critical limit (S_{cw}), the capability of the reservoir to conduct hydrocarbon will decrease quickly and the rock's ability to produce water will increase rapidly. This indicate the importance of evaluating the critical water saturation (S_{CW}).

In case of sandstone reservoirs, as in the case of AEB-3A reservoir, S_{cw} is a function of permeability (K) and effective porosity (Φe) (Fig. 13). Since the average permeability is 845 MD and the average effective porosity is 21%, the critical water saturation (S_{cw}) in this case is 29.5%. This means that AEB-3A reservoir in the study well will produce clean oil as the average S_w is 13%, which is much less than critical saturation (Table 2). Drill stem test (DST) results (Table 3) confirm this conclusion.

Minimum Bulk Volume of Water (BVW_{min}) The term minimum bulk volume water (BVW_{min}) refers to the minimum BVW value, at or below which the reservoir is expected to produce water-free hydrocarbons. Water-free production is required, because it costs money to extract and dispose the accompanied water.

BVW_{min} varies with lithology. For carbonate, it is about 3.5% and 5% for clean sandstone to as high as 14% for slightly shaly sandstone (Johnson and Kathryne 2006). Since S_w and Φ are the main parameters used for calculating water saturation, BVW_{min} can be calculated through rearrangement of Archie model as follows:

$$S_w^2 = \frac{Rw}{\Phi^2 \times Rt}$$

Rearrange this equation in terms of BVW yield

$$S_w^2 x\Phi^2 = \left(S_w x\Phi\right)^2 = (\text{BVW})^2 = \frac{\text{Rw}}{\text{Rt}}$$

$$\left(\text{BVW}_{\text{min}}\right)^2 = \frac{\text{Rw}}{\text{Rtmin}} \tag{8}$$

$$\text{Rt}_{\text{min}} = \frac{\text{Rw}}{(\text{BVWmin})^2}$$

The minimum true resistivity (RTmin) required for free-water production can be approximated according to matrix. In case of carbonate, it equals $800 \times R_w$. In case of clean

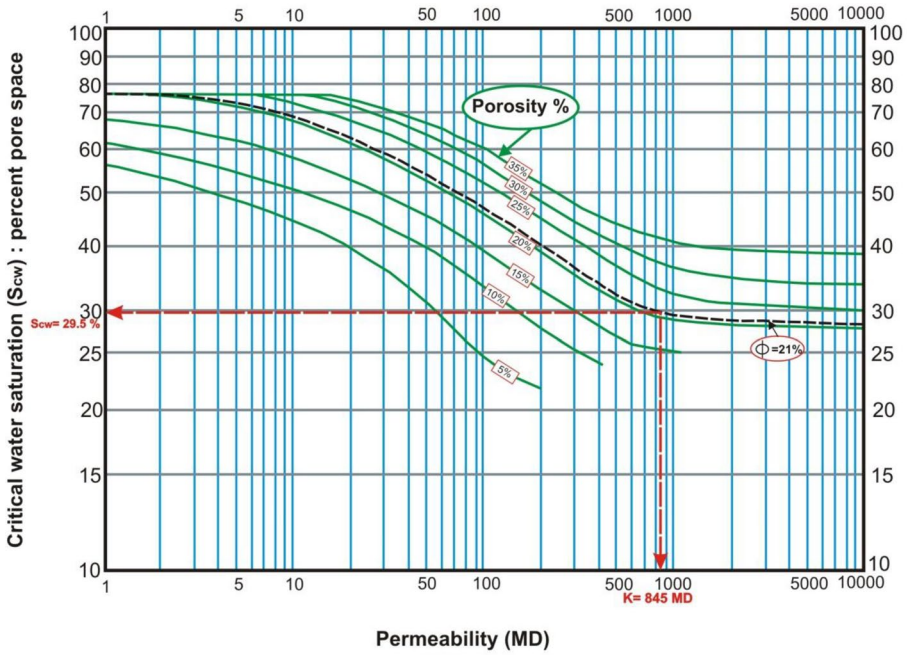

Fig. 13 Comparison of critical water saturation (Scw) with the porosity and permeability of tertiary's sand in the Gulf Coast (Granberry and Keelan, 1977; Bassiouni, 1994)

Table 2 BVWmin, Rtmin, Scw for the AEB-3A pay zone, Safir-03 well, Safir Field, North Western Desert

Well	Av. Rt (Ω.m)	Rtmin (Ω.m)	Av. Φe (%)	Av. Sw (%)	Scw (%)	Av. BVW	BVWmin
SAFIR-03	14	4	21	13	30	0.03	0.05

Table 3 Drill stem test (DST) data for the AEB-3A pay zone, Safir-N07and Safir-03 wells, Safir Field, North Western Desert (Khalda, Pet. Co.)

Well	Interval (Ft)	BFPD	BSW	BOPD	BWPD	GOR	Gas rate	WHFP
SAFIR-03	8108–8133	1350	0	1350	0	0	0	270

BFPD Barrel fluid per day, *BSW* Barrels water, *BOPD* Barrel oil per day, *BWPD* Barrel water per day, *GOR* Gas oil ratio and *WHFP* Well head formation pressure (psi)

sandstone, it equals $400 \times R_w$ and $200 \times R_w$ for slightly shaly sandstone. (Johnson and Kathryne 2006).

Applying this technique for AEB-3A pay interval, R_{tmin} equals 4 $\Omega.m^2/m$ (400×0.01) and BVW_{min} 0.05 (Eq. 8). The average values of the true resistivity (R_t) and BVW for this interval are 14 $\Omega.m^2/m$ and 0.03, respectively. Comparing these values with R_{tmin} and BVW_{min} (Table 2) clearly indicates water-free production as confirmed through the DST (Table 3).

Conclusions

Alam El Bueib Formation of the Lower Cretaceous age represents the major oil reservoir in Safir Field at Shushan Basin, northern Western Desert. Therefore, the current work aims to evaluate the quality of the sandstone reservoir of AEB-3A Member in Safir-03 well.

The formation evaluation of the Alam El Bueib 3A member from well logging data analysis indicates the presence of an oil-producing reservoir that has good quality between depths 8108–8133 ft. This reflects the net pay thickness of the AEB-3A sandstone reservoir in the studied borehole (well) amounts to 25 ft as indicated in Fig. 14. This reservoir characteristics show that the shale volume is less than or equal to 9%, which reflects a clean sandstone interval. It also displays low water saturation values (10–23%), interconnected porosity (19% to 23%), low BVW (≤ 0.04), irreducible water saturation (10–12%) and permeability 393–1339 MD, which reflects excellent reservoir quality. The calculated BVW_{min} of clean sandstone reservoir is 0.05, by comparing it with BVW values ($BVW_{min} > BVW$) clearly indicating hydrocarbon production will be water free as

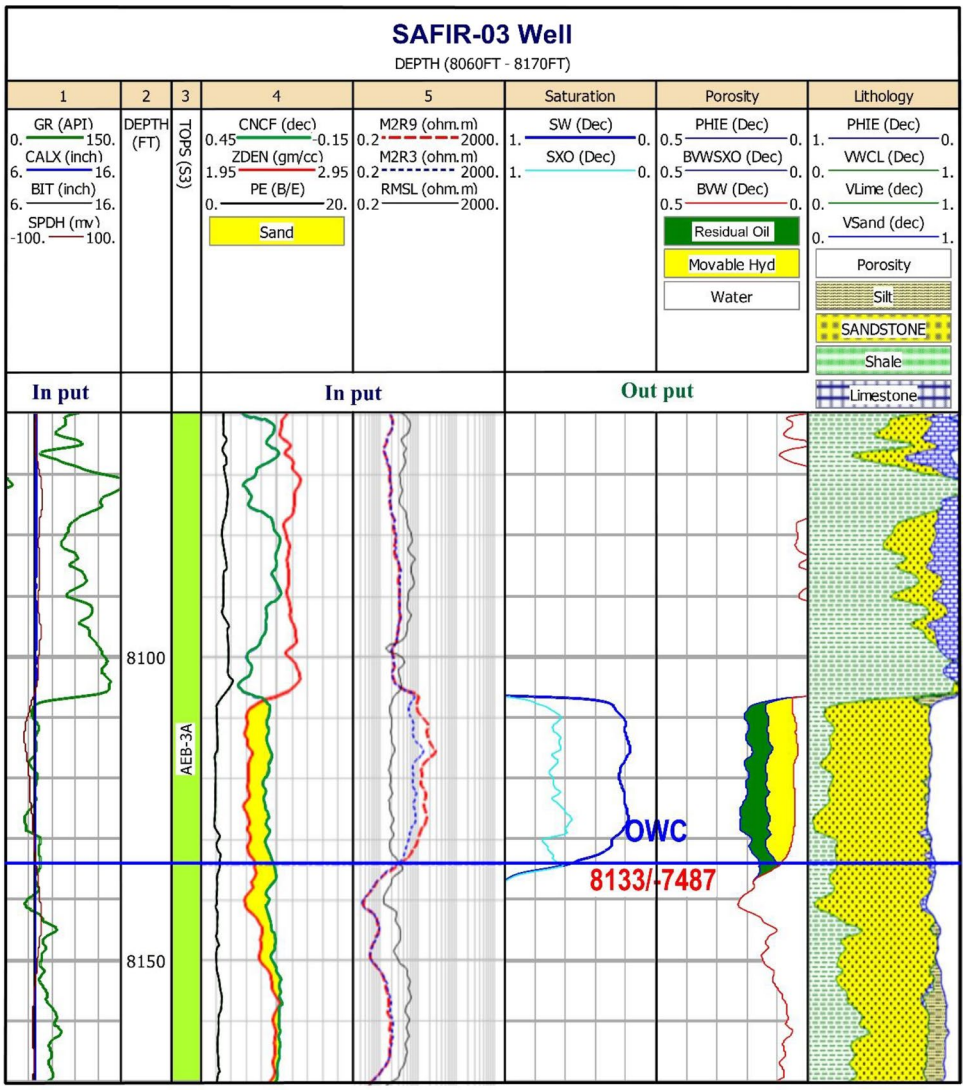

Fig. 14 Interpretation of the well-logging data of AEB-3A reservoir in Safir-03 well

confirmed through the DST. The relative permeabilities for water and oil (K_{rw} and K_{ro}, respectively), which have been calculated based on S_w and S_{wirr} cross-plots, clearly indicate good reservoir quality because the plurality of points is situated between 0.01 and 0 K_{rw} and located between 1.0 and 0.5 K_{ro} for AEB-3A sandstone reservoir. Also, the zero points of K_{rw} are plotted on and below 1.0 K_{ro} line, which reflects 100% and 0% relative permeabilities to oil and water, respectively. On the other hand, the water cut of water production of the AEB-3A Member is quite low (0–20%).

The critical water saturation (S_{cw}) for net pay AEB-3A sandstone reservoir is 29.5%, while the average of the calculated water saturation values for this pay is 13% (i.e., $S_w < S_{cw}$). So, it is reflected that the total net pay will flow oil, whereas the water phase will remain immobile. This is confirmed with reservoir engineering through the DST.

Acknowledgements The authors are grateful to the Egyptian General Petroleum Corporation (EGPC) and Khalda Petroleum Company (KPC), for providing the data for this research.

Funding There was no funding resources available during the processing and produce this work.

Open Access This article is licensed under a Creative Commons Attribution 4.0 International License, which permits use, sharing, adaptation, distribution and reproduction in any medium or format, as long as you give appropriate credit to the original author(s) and the source, provide a link to the Creative Commons licence, and indicate if changes were made. The images or other third party material in this article are included in the article's Creative Commons licence, unless indicated otherwise in a credit line to the material. If material is not included in the article's Creative Commons licence and your intended use is not permitted by statutory regulation or exceeds the permitted use, you will need to obtain permission directly from the copyright holder. To view a copy of this licence, visit http://creativecommons.org/licenses/by/4.0/.

References

Alsharhan AS, Abd El-Gawad EA (2008) Geochemical characterization of potential Jurassic/Cretaceous source rocks in the Shushan Basin, north Western Desert. Egypt J Pet Geol 31(2):191–212

Archie GE (1942) The electrical resistivity log as an aid in determining some reservoir characteristics. Petrol Technol 5:54–62

Asquith G, Gibson C (1982) Basic well log analysis for geologists: methods in exploration series. AAPG, Tulsa, Oklahoma

Asquith GB, Krygowski D, Gibson CR (2004) Basic well log analysis, vol 16. AAPG, Tulsa

Bassiouni Z (1994) Theory, measurements, and interpretation of well logs. SPE Printed, USA

Buckles RS (1965) Correlating and averaging connate water saturation data. J Can Pet Technol 4(1):42–52

EGPC (1992) Western Desert, oil and gas fields, a comprehensive overview. In: 11th petroleum exploration and production conference. Egyptian General Petroleum Corporation, Cairo

El Shazly EM (1977) The geology of the Egyptian region. In: Stehli FG (ed) The ocean basins and margins, Kanes, . AEM FG Plenum, New York

Granberry RJ, Keelan DK (1977) Critical Water Estimates for Gulf Coast Sands, trans. Gulf Coast assn. of Geologic Scientists, P 27

Hantar G (1990) North western desert. In: Said R (ed) The Geology of Egypt. Brookfield, Rotterdam

Johnson DE, Kathryne EP (2006) Well logging in nontechnical language, 2nd edn. Pennwell Corporation, OklahomA

Khalda Pet. Co. Khalda petroleum company internal reports. Cairo, Egypt

Metwalli FI, Pigott JD (2005) Analysis of petroleum system criticals of the Matruh-Shushan Basin, Western Desert. Egypt Petroleum Geosci 11:157–178

Moustafa AR (2008) Mesozoice Cenozoic basin evolution in the northern Western Desert of Egypt. In: Salem, M., El-Arnauti, A., Saleh, A. (Eds.), 3rd Symposium on the Sedimentary Basins of Libya, The Geology of East Libya

Pickett GR (1972) Practical formation evaluation. G.R Pickett Inc, Golden

Said R (1962) The geology of Egypt. Elsevier Publ. Co., Amsterdam

Said R (1990) (Ed) The Geology of Egypt. A.A. Balkema, Rotterdam, Book field, published for the EGPC, CONOCO Hurghada Inc., and REPSOL Exploration, S.A., 734 p

Sarhan MA (2017) Wrench tectonics of Abu Gharadig Basin, Western Desert, Egypt: a structural analysis for hydrocarbon prospects. Arab J Geosci 10(18):399

Sarhan MA, Collier REL (2018) Distinguishing rift-related from inversion-related anticlines: observations from the Abu Gharadig and Gindi Basins, Western Desert. Egypt J Afr Earth Sci 145:234–245

Sarhan MA, Basal AMK, Ibrahim IM (2017a) Seismic and well logging interpretation for evaluation of the lower Bahariya reservoir, southwest Qarun (SWQ) Field, Gindi Basin. Egypt Mar Geophys Res 38(3):271–290

Sarhan MA, Basal AMK, Ibrahim IM (2017b) Integration of seismic interpretation and well logging analysis of Abu Roash D Member, Gindi Basin, Egypt: implication for detecting and evaluating fractured carbonate reservoirs. J Afr Earth Sci 135:1–13

Sarhan MA (2019) Seismic delineation and well logging evaluation for AlbianKharita formation, South West Qarun (SWQ) Field, Gindi Basin. Egypt J Afr Earth Sci 158(2019):103544

Schlumberger (1972) Log interpretation/charts. Schlumberger Well Services Inc, Houston

Schlumberger (1986) Log Interpretation Manual/charts

Schlumberger (1995) Well Evaluation Conference, Cairo, Egypt, 87

Shalaby MR, Hakimi MH, Abdullah WH (2012) Organic geochemical characteristics and interpreted depositional environment of the Khatatba Formation, northern Western Desert. Egypt Am Assoc Pet Geol Bull 96(11):2019–2036

Shalaby MR, Hakimi MH, Abdullah WH (2014) Petroleum system analysis of the Khatatba Formation in the Shoushan Basin, north Western Desert. Egypt Arab J Geosci 7:4303–4320

Timur A (1968) An investigation of permeability, porosity, and residual water saturation relationships. In: SPWLA 9th Annual Logging Symposium. Society of Petrophysicists and Well-Log Analysts

Publisher's Note Springer Nature remains neutral with regard to jurisdictional claims in published maps and institutional affiliations.